NASA TN D-1515

TECHNICAL NOTE

D-1515

SIMULATOR STUDY OF AN ACTIVE CONTROL SYSTEM FOR A SPINNING BODY

By James J. Adams

Langley Research Center
Langley Station, Hampton, Va.

NATIONAL AERONAUTICS AND SPACE ADMINISTRATION
WASHINGTON

December 1962

NATIONAL AERONAUTICS AND SPACE ADMINISTRATION

TECHNICAL NOTE D-1515

SIMULATOR STUDY OF AN ACTIVE CONTROL SYSTEM FOR A SPINNING BODY

By James J. Adams

SUMMARY

Model simulator tests of an automatic precession-wheel damping controller for a spinning vehicle have been made by using an inertial simulator mounted on an air bearing. The control system provides the necessary control torques through the use of a spinning wheel, which provides precession torques. The wheel position is commanded by an automatic closed-loop servomechanism system which uses rate gyros to provide the command signals. The results show that this type of controller provides very good wobble damping and also provides the torque necessary to keep the vehicle spinning on its body axis of symmetry in the presence of a shift in the principal axes. These tests also show that linear equations of motion provide a good prediction of the performance of the controller. The tests were made with the simulator in disk-, sphere-, and rod-shaped configurations.

INTRODUCTION

In reference 1 a theoretical study was made of a scheme for automatically controlling the nutation, or wobble, motion of a spinning vehicle. The problem of special interest treated in this study was the problem peculiar to a rotating manned space station in which the movement of the occupants would cause a change in the dynamic balance of the station, by causing the principal axes to shift, which would result in a wobble motion of the station. In the example given in reference 1, it was shown that a reasonable change in product of inertia resulted in a maximum attitude change of 12° and a corresponding variation in body-axis rates of rotation. It was also shown that a spinning wheel used for control could reduce this motion to a steady 0.5° attitude change.

The results of the analytical study of reference 1 were so encouraging that further research in the form of tests with an experimental model of the system were made to provide a more complete check of the theory. The analytical study included many simplifying assumptions, of course. These simplifications included the assumption of perfect servo operation, the omission of several second-order terms for rigid-body motion, and the omission of several second-order effects of the controller, such as that due to the inertia of the controller gimbals and all momentums of the controller mechanism except that produced by the control wheel.

The effects of misalinement and drift of the sensor and unforeseeable nonlinearities in the control system were also neglected. Therefore, tests with a small-scale dynamic simulator were made to check these factors.

SYMBOLS

c	displacement of principal axes from body axes, deg
H	control-wheel momentum, ft-lb-sec
H_X, H_Y, H_Z	components of control-wheel momentum along X-, Y-, and Z-axis, respectively, ft-lb-sec
I_X, I_Y, I_Z	moments of inertia about X-, Y-, and Z-axis, respectively, slug-ft^2
I_{XY}	product of inertia, slug-ft^2
K	damping gain, deg/deg/sec
m,n	displacement of body axis of symmetry from reference line in XY- and XZ-plane, respectively, deg
p,q,r	rates of rotation on X-, Y-, and Z-axis, respectively, deg/sec
X,Y,Z	body axes (X-axis is axis of symmetry)
δ_Y, δ_Z	deflections of inner and outer gimbals, respectively, deg

Positive directions are as defined by a right-hand axis system.

DESCRIPTION OF CONTROL SYSTEM AND SIMULATOR

The control torques used in the control system were the precession torques produced by a spinning wheel. Precession torques arise when a spinning wheel is forced to rotate about an axis other than its spin axis. A sketch is shown in figure 1 of the controller configuration that was used to achieve this type of application for a spinning vehicle. The control wheel, which spins at a constant rate, is mounted in a double-gimbal arrangement. The operation of the mechanism is as follows. When no torque is required, the control-wheel angular momentum vector H is alined with the spin vector of the vehicle. When torque is required about a particular body axis of the vehicle, the control wheel is rotated on an axis parallel to that body axis; thereby, a component of the control-wheel angular momentum vector is produced along an axis that is perpendicular to both the vehicle spin vector and the vehicle body axis for which the torque is required. This arrangement of the vectors produces the desired torque. For example (see fig. 1(b)), if a torque is required on the Z body axis, a gimbal deflection δ_Z

is commanded which produces the momentum component H_Y. Similarly, if a torque is required on the Y body axis, a gimbal deflection δ_Y is commanded which produces the momentum component H_Z. The torque produced is a nearly proportional function of the tilt of the control wheel.

The gimbal deflections are commanded proportional to rate-gyro signals to provide damping to the system. A block diagram of the control system used to achieve this relation is shown in figure 1. In some cases, signals from a light sensor were also used to command gimbal deflections to provide extra attitude stiffness to the vehicle momentum vector.

A photograph of the simulator is shown in figure 2, and additional information is given in the following table:

	$\frac{I_Y}{I_X} = 0.76$	$\frac{I_Y}{I_X} = 0.91$	$\frac{I_Y}{I_X} = 1.25$
Weight, lb	269	287	329
I_X, slug-ft^2	8.63	8.82	9.33
I_Y or I_Z, slug-ft^2	6.55	8.05	11.7
c (movable weight displaced), deg	-3.35	-8.6	2.96
I_{XY} (movable weight displaced), slug-ft^2	0.122	0.122	0.122

The simulator consisted of a very rigidly constructed platform mounted on a 6-inch-diameter spherical air bearing. The simulator could rotate approximately $\pm 20^\circ$ about the horizontal axes Y and Z and had unlimited freedom on the spin axis X. Tests showed that the drag moment on the platform at 30 rpm was 0.04 foot-pound, which caused an exponential decay in the spin angular velocity. For example, the spin rate would change from 30 rpm to 20 rpm in $3\frac{1}{2}$ minutes.

A light sensor, mounted at the top of the simulator, measured the deflection of the two-horizontal body axes from a vertical reference line generated by a 500-watt light mounted above the simulator and simulating the sun. Photoresistive light cells were used in the light sensor to produce direct-current signals. These signals were amplified in transistor amplifiers, and the output was recorded and, in some cases, used in the control system. Two orthogonal miniature precision rate gyros were mounted on the platform to measure rates of rotation of the body axes perpendicular to the body axis of symmetry. The gyro spin momentum vectors were pointed in the same direction as the platform spin momentum vector. This arrangement eliminated the divergent moment that would occur on the gyros when they were deflected. However, this arrangement caused the sensitivity of the rate gyros to be reduced by approximately 10 percent. The gyros had a maximum range of ± 20 degrees per second and a hysteresis limit of 0.001 of full scale. Power for the gyros was supplied by a solid-state inverter. The 400-cycle output signal of each of the gyros was demodulated and amplified with transistor amplifiers, and

the output was used in the control system. The output was also recorded and is shown in the figures as q and r.

The control wheel in its double-gimbal mount is shown in figure 2 at the front part of the simulator in a deflected position. The gimbal positions were controlled by permanent-magnet direct-current motors directly connected to the gimbals. No gears were used in the motor drive. An angular potentiometer was located on each gimbal axis. The sensor signals were summed with these gimbal-angle signals to form the error-signal input to the gimbal-servomotor power amplifiers. These power amplifiers were high-gain units with limited outputs. Records of both the inner and outer gimbal position in response to step input signals calling for 10° gimbal deflections are shown in figure 3. It can be seen that the response provided by the gimbal system is very fast and well damped. The inner gimbal reached a steady deflection in 0.05 second, and the outer gimbal, in 0.15 second. The maximum slewing rate of the inner gimbal was 850 degrees per second, and of the outer gimbal, 260 degrees per second. Gimbal deflection was limited to 90°.

The gains of both the rate-gyro signals and the light-sensor signals were adjustable. The rate-gyro signals could be adjusted so that up to 12° of gimbal deflection per degree per second of the simulator rotation rate on the Y- and Z-axis would result. Variations in this ratio resulted in changes in the damping of the controlled system. Therefore, this ratio is called the damping gain and is expressed in the reduced unit of seconds. The light-sensor gains could be varied up to 16° of gimbal deflection per degree of simulator tilt.

The control-wheel rate of rotation could be varied from 2,500 rpm to 4,650 rpm. A tachometer feedback signal was used to regulate the control-wheel speed, which was held constant at 4,650 rpm for all tests reported in this paper. The wheel had an inertia of 1.04×10^{-3} slug-ft^2.

The light-sensor and rate-gyro signals were recorded on a four-channel pen recorder mounted on the simulator.

In order to simulate the movement of an occupant of a manned space station, two movable weights were mounted on opposite sides of the simulator. One weight moved upward while the other moved downward so as to maintain static balance while the dynamic balance was being changed. These weights, weighing 2.83 pounds each, were located 16 inches from the center of the simulator and moved 6.25 inches parallel to the simulator symmetrical axis when activated, creating a product of inertia of 0.122 slug-ft^2. The simulator was dynamically balanced so that the principal axes coincided with the body axes when the movable weights were in their nominal initial position. When activated they would complete their movement in approximately 10 seconds. The location of the weights was such that when they were displaced, a deflection of the inner gimbal of the controller was required in order to supply a torque to oppose the steady unbalance torque.

The spin-up mechanism, which is the overhead arm with a small motor attached, is shown in place in the photograph in figure 2. When the desired spin rate of the simulator was established, the spin-up motor was disengaged from the simulator and the overhead arm was swung out of the way, leaving the simulator free to move.

The inertia ratio of the simulator, the ratio of the moment of inertia of the two horizontal axes to the moment of inertia of the spin axis, was varied by adding weights to the top and bottom of the simulator. The inertia configuration could be varied between the limits of a near disk, $I_Y/I_X = 0.76$, and a rod, $I_Y/I_X = 1.25$. These weights which were added were symmetrically shaped and did not change the directions of the principal axes.

RESULTS AND DISCUSSION

The results of tests made with the simulator in the near-disk configuration, $I_Y/I_X = 0.76$, are shown in figure 4. In these runs the movable weights were initially set in their displaced position, which produced the effect of a step change in product of inertia to be applied to the simulator when it was released at the start of a test run. Figure 4(a) shows the resulting response with the controller in operation with a damping gain of 1 second. The response is a damped oscillation in q and r with a time to half-amplitude of 2.5 or 3 seconds. The quantities m and n are the respective angular displacements of the body axis of symmetry in the XY and XZ planes from the fixed reference line established by the simulated sun. In these tests, no attempt was made to have the simulator pointing directly at the reference light at the start of a run; therefore, m and n contain a cyclic variation, with a frequency corresponding to the spin rate, superimposed on the variation due to the wobble motion. The spin rate was 108 degrees per second (18 rpm) in this test. This initial displacement from the sun reference line varied from run to run.

With the damping gain of 1 second, as was used in the test shown in figure 4(a), only small deflections of the controller gimbals were called for; thus, full utilization of the controller was not made. Therefore, additional tests were made with gains of 5 seconds and 12 seconds, and results of these tests are shown in figures 4(b) and 4(c). With the higher gains more damping was provided, and the responses showed very rapid, deadbeat reductions to the steady-state values.

Similar tests, with damping gains of 1, 5, and 12 seconds, were made with the simulator in the near-sphere configuration, $I_Y/I_X = 0.91$, and the results are shown in figure 5; test results for a near-rod configuration, $I_Y/I_X = 1.25$, are shown in figure 6. These tests also show that very good damping is provided by the controller. Expected variations in the steady-state values and period of oscillation occurred in these tests because of the changes in inertia ratio. These factors will be discussed in detail in a subsequent section.

The damping characteristics of the controller are summarized and compared with calculated values in figure 7. The calculated values were obtained by using the linear equations presented in reference 1 and by using inertia values and spin rates that apply to the experimental tests. The calculations were extrapolated up to a value of I_Y/I_X of 2. All results presented in figure 7 are for a damping gain of 1 second. Very good damping is provided for all configurations tested, even with the low control gain of 1 second. Good agreement exists between the experimental and calculated results, and this agreement gives confidence that the

performance for a particular design can be adequately predicted with the equations of motion presented in reference 1.

With control gains higher than 1 second the damping was improved. In addition to the increase in the damping, the advantage of using the higher gains was a reduction in the steady-state velocity error. For the case of a spinning body, such as the one of this investigation, the most graphic way of describing this steady-state velocity error is to refer to it in terms of the angle of the cone generated by the body axis of symmetry. The constant unbalanced torque created by the constant dynamic unbalance, which was the disturbance used in these tests, resulted in the vehicle body axis of symmetry moving so as to trace a cone after the transient had been eliminated. With very low damping gain, the half-angle of the cone was equal to the displacement of the principal axes from the body axes corresponding to the dynamic unbalance, or product of inertia. A plot of the steady-state cone half-angle as a function of damping gain for the nearly spherical configuration $\left(I_Y/I_X = 0.91\right)$ is shown in figure 8. The cone half-angle was determined by the relationship

$$\text{Cone half-angle} = \tan^{-1} \frac{\sqrt{r^2 + q^2}}{p}$$

For this configuration the displacement of the principal axes from the body axes corresponding to the product of inertia created by the movable weights was 8.6°. With a damping gain of 1 second the steady-state cone half-angle was 5°, and with a damping gain of 12 seconds it was 1°. Therefore, if it is necessary to keep the vehicle spinning on the body axis of symmetry while the mass distribution of the vehicle may be changing, the precession-wheel controller provides a means for accomplishing this end. The accuracy of the alinement is a function of the dynamic unbalance, on one hand, and of the size and the damping gain of the controller, on the other.

Several other minor points of agreement between the experimental and calculated results that were noted will now be discussed. Some additional test runs made with the near-disk configuration are shown in figure 9. Figure 9(a) shows the response of the uncontrolled simulator when the simulator was initially spun on the body axis of symmetry with the movable weights displaced. The calculated wobble period for this configuration is 10.5 seconds, and the measured period of 10 seconds checks very well. It was shown in reference 1 that the maximum value of body angular rate q_{max} that would occur in this situation is related to the displacement of the principal axes from the body axes and the spin rate by the formula

$$q_{max} = p \tan 2c$$

The angle c can be obtained by the formula

$$\tan 2c = \frac{-2I_{XY}}{I_X - I_Y}$$

For the near-disk configuration with the movable weights displaced (I_{XY} = 0.122 slug-ft^2), the angle c was -3.35°. The calculated maximum value of q, based on a measured spin rate of 108 degrees per second, was 12.6 degrees per second, and the measured value was approximately 12 degrees per second.

Of interest is the variation in the response of the simulator in the near-disk configuration with the movable weights displaced, but with the control wheel spinning and with the gimbals locked in position. In this case the control wheel added no control, but added an increment of momentum to the simulator spin momentum and effectively increased the spin moment of inertia I_X of the simulator. This change in I_X reduced the calculated wobble period of 9.35 seconds, and the calculated maximum value for q was 10 degrees per second. The measured results show that these trends were followed in the experiments. (See fig. 9(b).) The measured wobble period was 8.7 seconds, and the measured maximum value of q was approximately 10 degrees per second.

Figure 9(c) shows a time history of simulator response to a programed series of events. In these tests the simulator principal axes were initially alined with the body axes, and the simulator started spinning on the symmetrical axis. The control-wheel spin rate was established before the start of the run at 4,650 rpm. A few seconds after the start of the run the movable weights were moved, and a change in I_{XY} from 0 to 0.122 slug-ft^2 resulted. The movement of the weights required approximately 10 seconds. One minute after the weights moved the control wheel was uncaged and set operating. The damping gain was 12 seconds. The result of this ramp change in the product of inertia in this test as contrasted to the step change in disturbance used in tests shown in figure 9(a) was a smaller variation in the measured parameters q, r, m, and n. When the gimbals were uncaged, the wobble was quickly eliminated.

Similar tests at an inertia ratio of 0.91 are shown in figure 10. The calculated period of the wobble motion for the uncontrolled test was 33.4 seconds, and the measured period was 29 seconds. Since the recorded variation in q went off the recorder scale in this run, it is more convenient to compare calculated and measured values of r. The displacement of the principal axes was -8.6° in this case, and the calculated maximum value of r was 16 degrees per second, which can be compared to the measured value of approximately 12 degrees per second. The effect of having the wheel spinning, but caged, was again a reduction in the amplitudes of q and r (fig. 10(b)), and the effect of having the weights move with a ramp variation was a further reduction in the amplitudes of q and r (fig. 10(c)).

Tests at an inertia ratio of 1.25 (fig. 11) gave positive values of q, which is in agreement with the results given in reference 1. (For the previous tests, q was negative.) The calculated period was 22.5 seconds whereas the measured value was 20 seconds. The displacement of the principal axis was 2.96° in this case. The calculated maximum value of q was 11.4 degrees per second, and the measured value was approximately 10 degrees per second.

The addition of the spinning control wheel with the gimbals caged caused an increase in the period of the wobble motion in these tests on the rod-shaped

configuration. As anticipated, this increase is opposite to the effect noted for the disk. The amplitudes of q and r are increased, also, and the further effect of the ramp change in the mass distribution was a reduction in the amplitudes of q and r. The two effects cancelled each other in these tests.

It was suggested in reference 1 that the addition of the light-sensor signals to the control system would result in a convergence of the X body axis towards the reference direction as established by the reference light. However, it is now realized that this theory is incorrect. The addition of the light-sensor signals reduces an initial attitude error due to a misalinement of the momentum vector of the vehicle, but does not bring about a convergence towards the reference line. This reduction is brought about because the light-sensor signals cause the control-wheel momentum vector to turn away from the reference, which in turn causes the vehicle momentum vector to turn towards the reference line. The vector sum of the two momentum vectors is therefore unchanged with respect to inertial space. Figure 12 shows an example of the attitude correction in which the simulator was started spinning with a displacement of the X body axis from the reference line of approximately 3°, as is indicated by the amplitude of the variation in m and n at the spin frequency. There was some wobble motion present initially, and the controller was initially caged in this test. When the controller was uncaged, the wobble motion was eliminated, and the simulator momentum-vector displacement was reduced to approximately 2°. The damping gain was 12 seconds and the light-sensor gain was 16 in this test.

CONCLUDING REMARKS

Tests made on an automatic precession-wheel damping controller for a spinning vehicle indicate that the controller provides very good wobble damping. The controller also keeps the vehicle spinning on its body axis of symmetry in the presence of a shift in the principal axes. Some correction to an initial misalinement of the vehicle momentum vector from an inertial reference line is also possible with the controller.

The good agreement between calculated and measured damping performance indicates that linear equations of motion can be used to predict the performance of such a control system.

Langley Research Center,
National Aeronautics and Space Administration,
Langley Station, Hampton, Va., September 4, 1962.

REFERENCE

1. Adams, J. J.: Study of an Active Control System for a Spinning Body. NASA TN D-905, 1961.

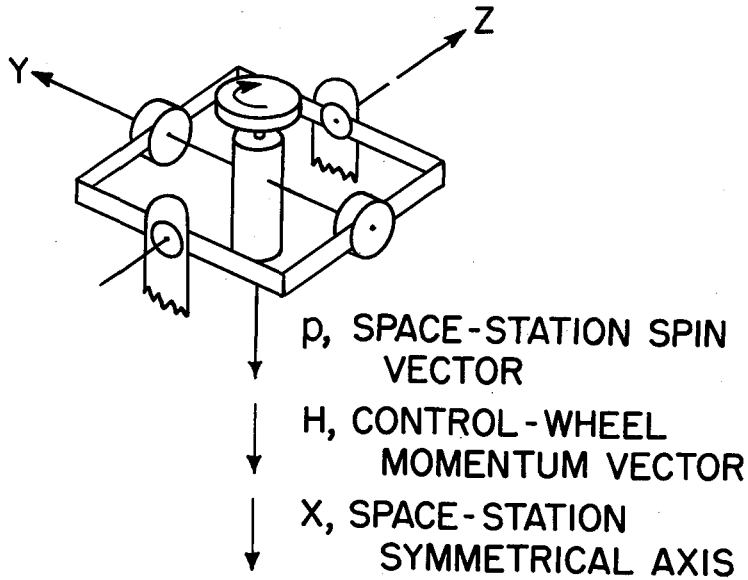

(a) Zero-torque position.

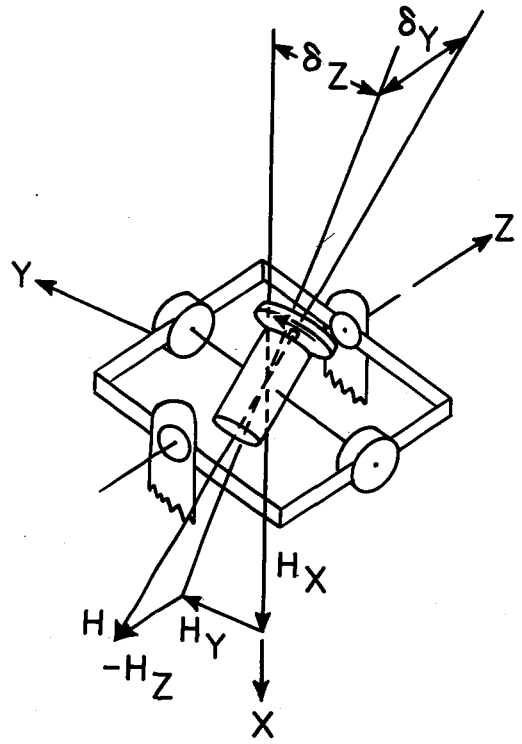

(b) Deflected position.

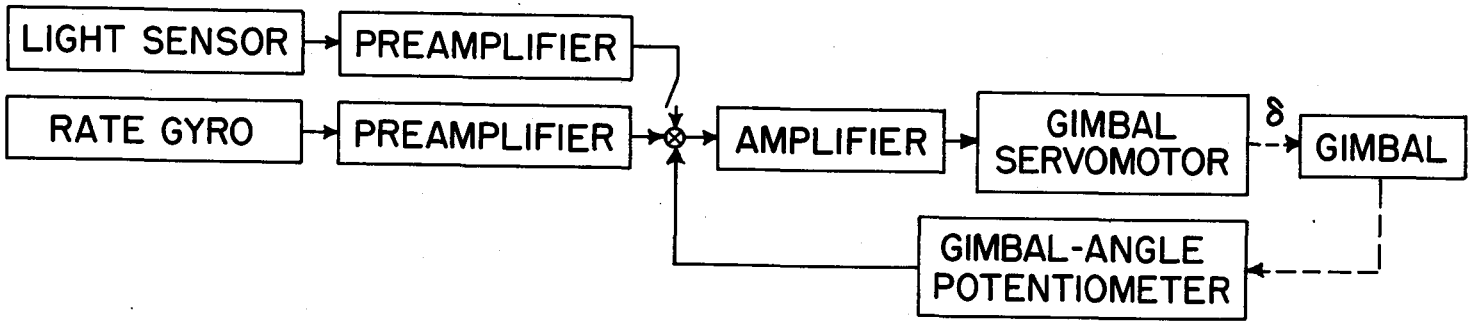

(c) Block diagram for one axis.

Figure 1.- Sketch of controller.

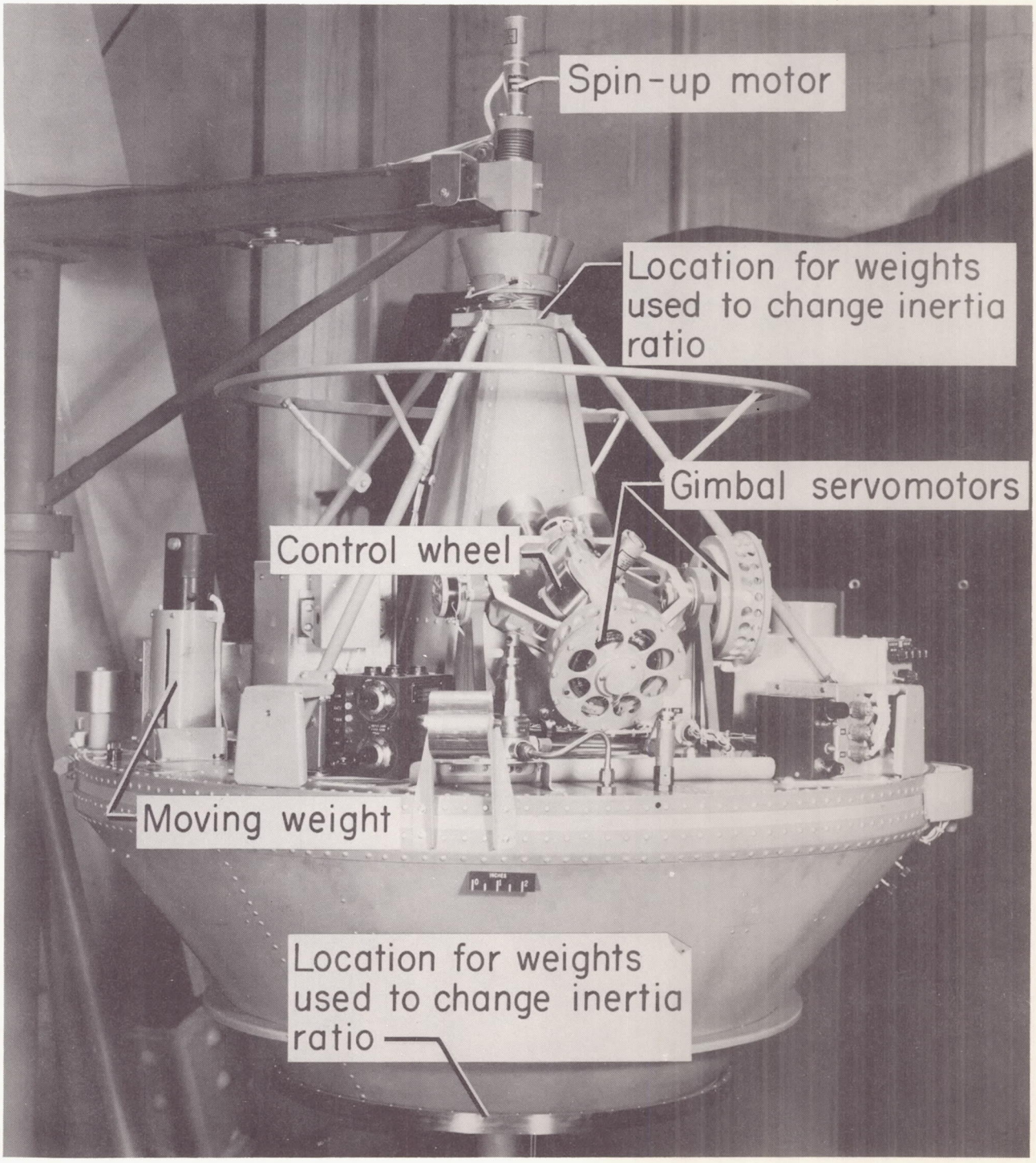

Figure 2.- Photograph of simulator. L-62-2141

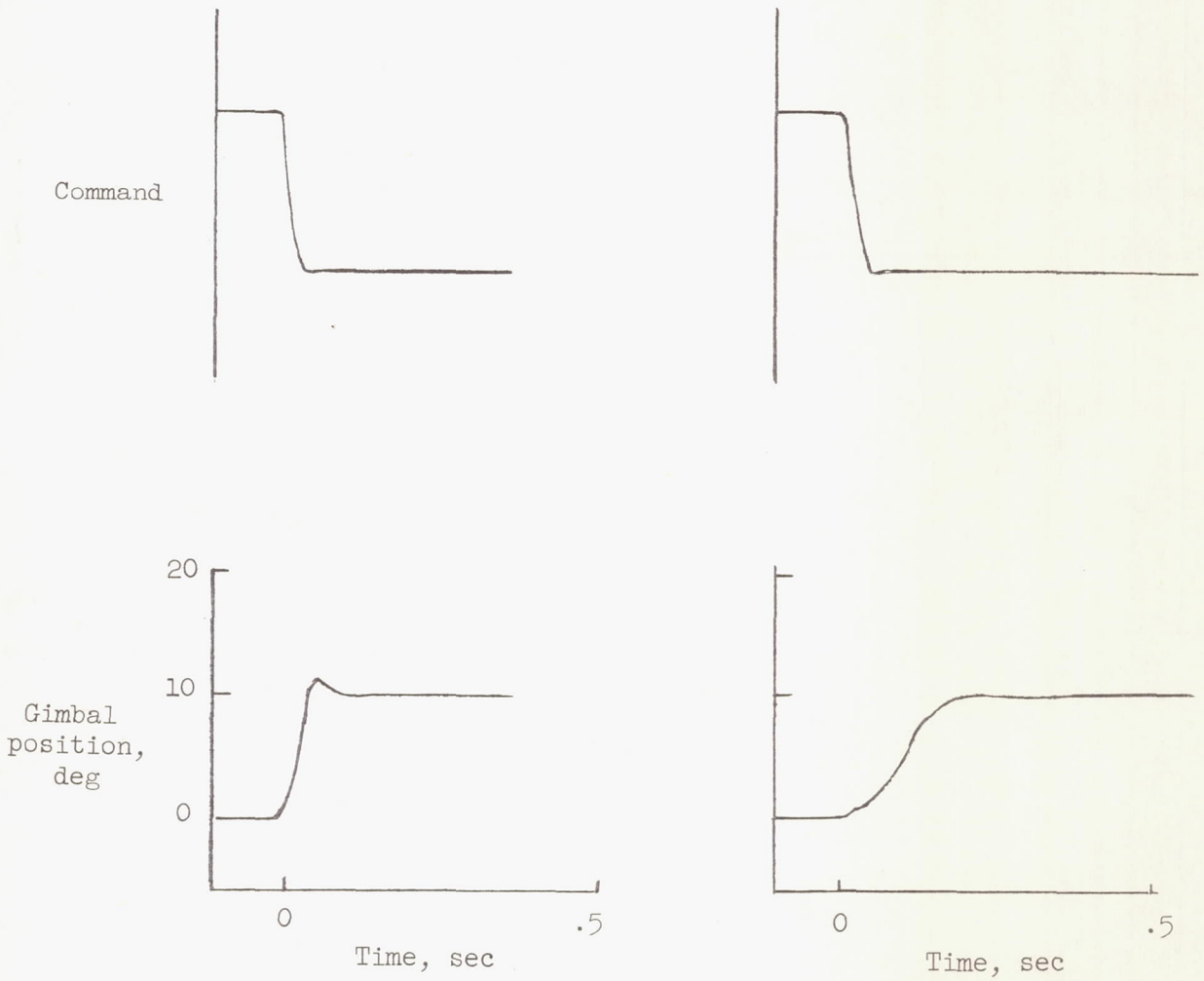

(a) Inner gimbal.

(b) Outer gimbal.

Figure 3.- Gimbal response.

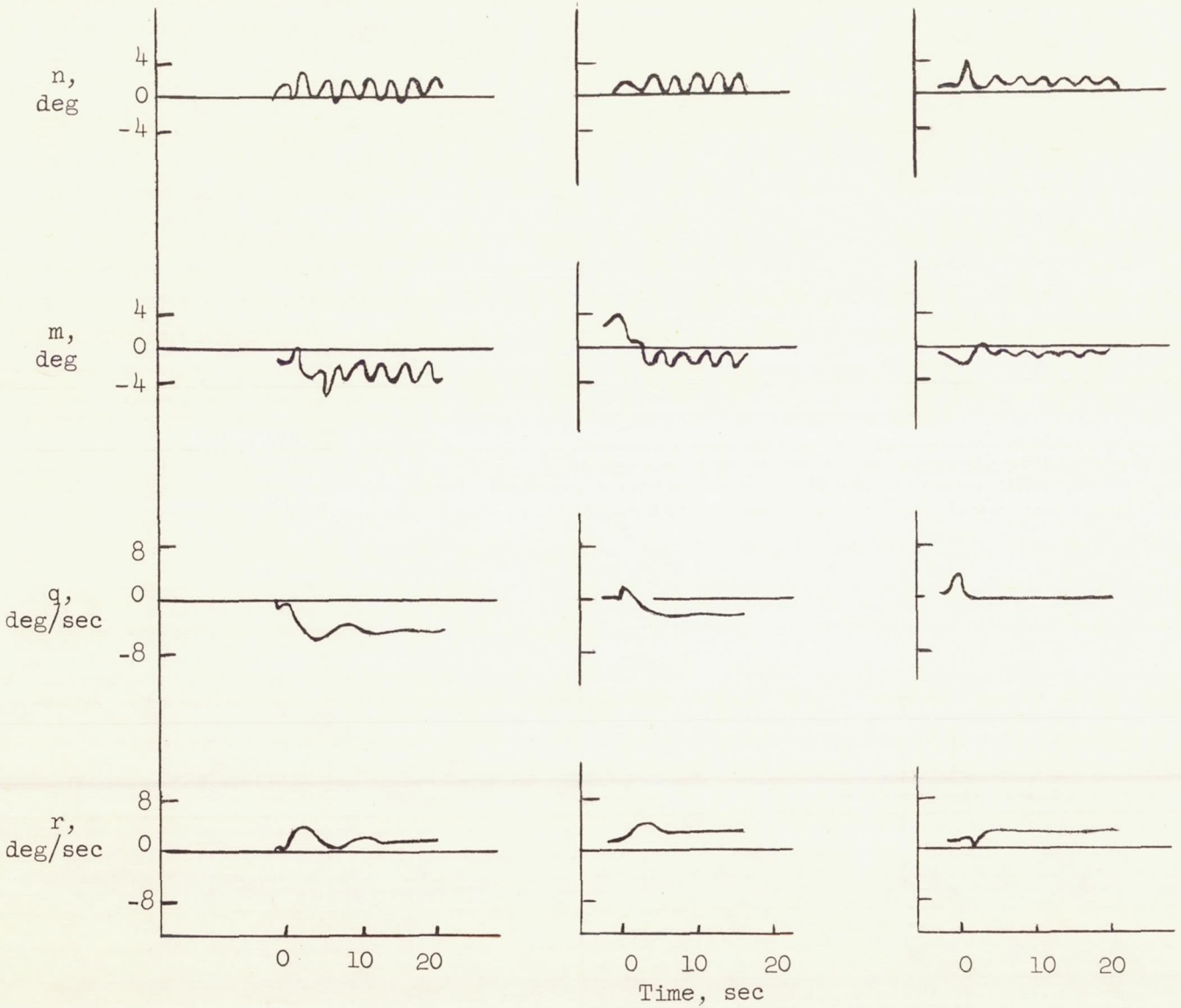

(a) K = 1 second. (b) K = 5 seconds. (c) K = 12 seconds.

Figure 4.- Response of simulator with $I_Y/I_X = 0.76$. Simulator dynamically unbalanced at start of runs.

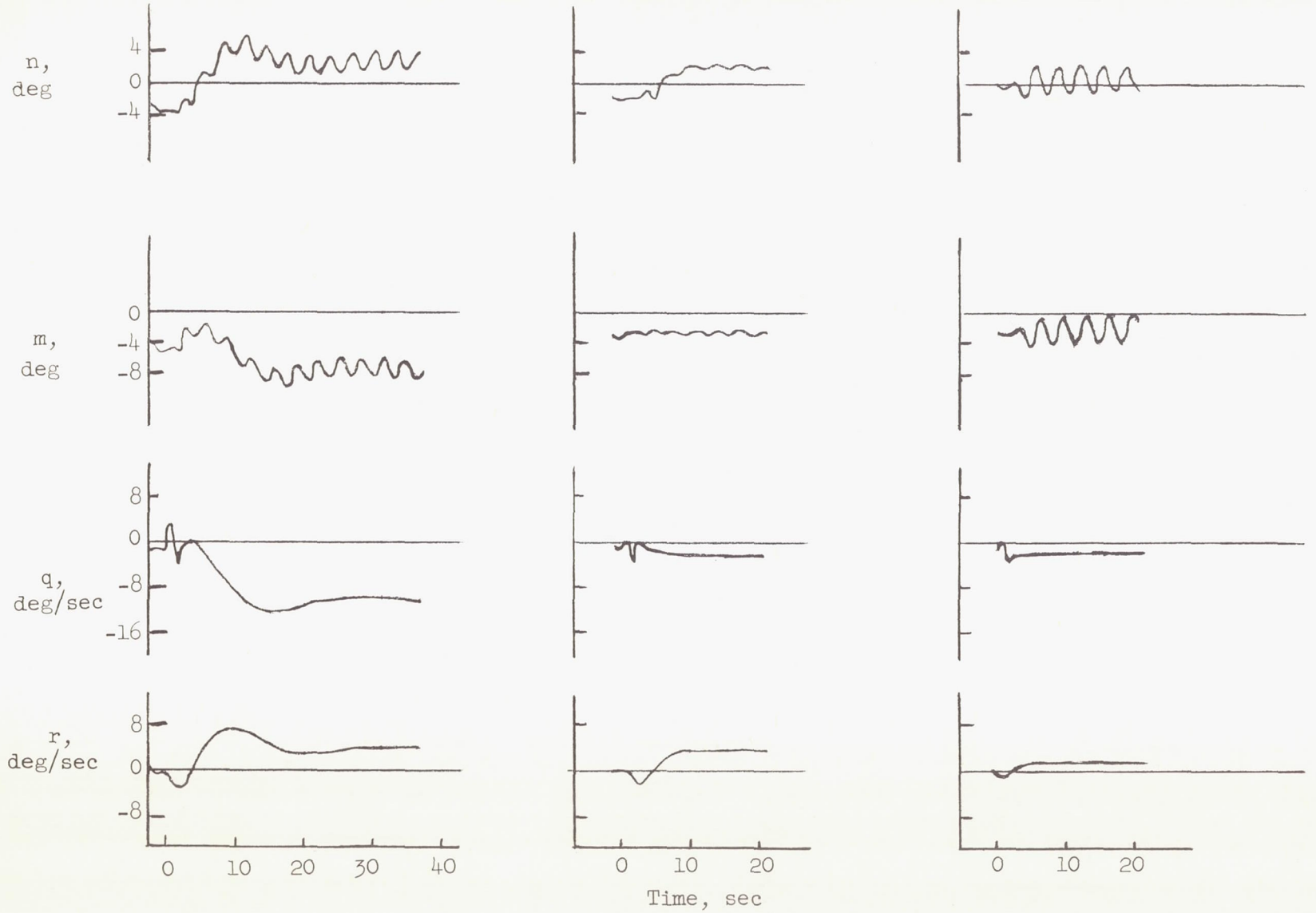

(a) K = 1 second. (b) K = 5 seconds. (c) K = 12 seconds.

Figure 5.- Response of simulator with $I_Y/I_X = 0.91$. Simulator dynamically unbalanced at start of runs.

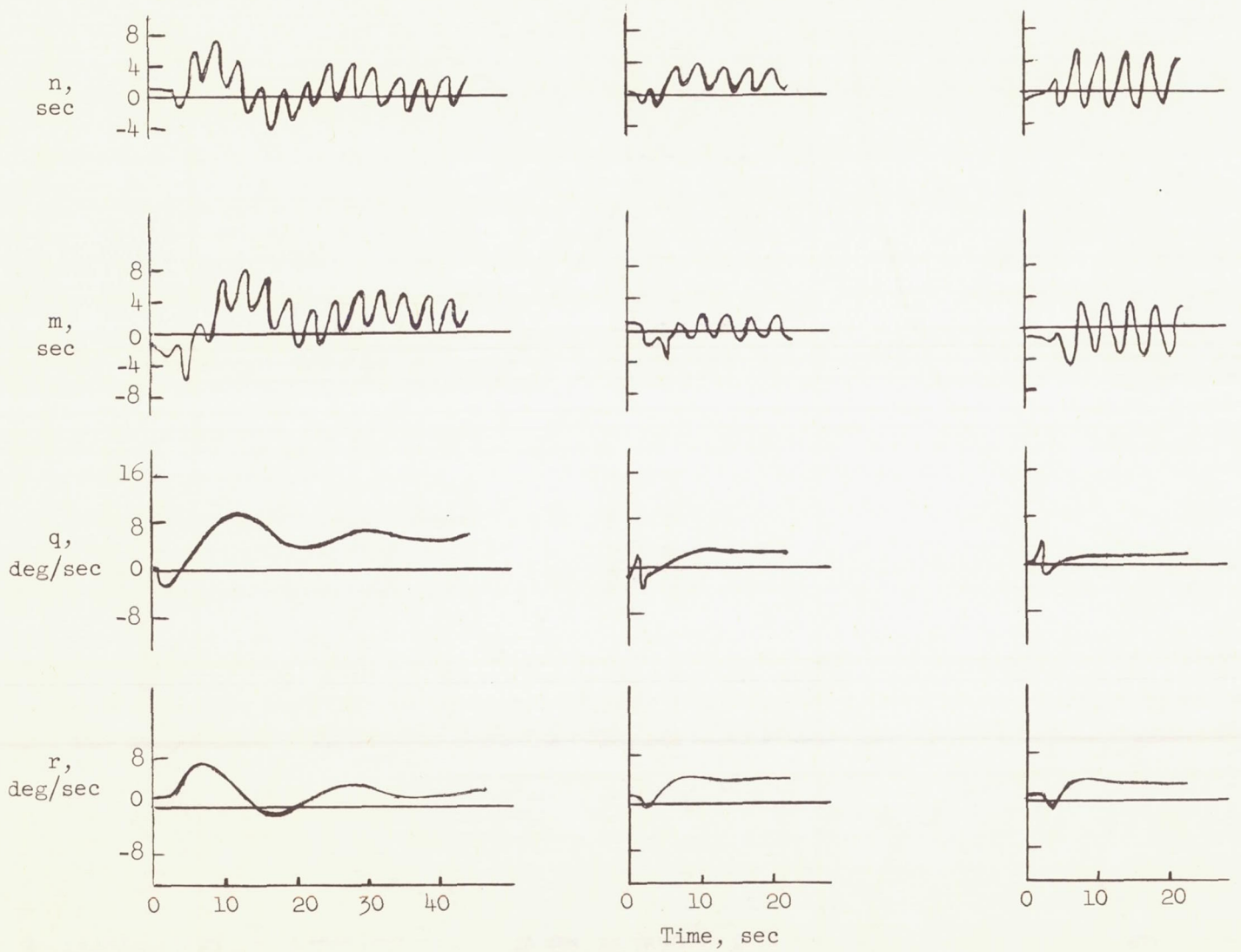

(a) K = 1 second. (b) K = 5 seconds. (c) K = 12 seconds.

Figure 6.- Response of simulator with $I_Y/I_X = 1.25$. Simulator dynamically unbalanced at start of runs.

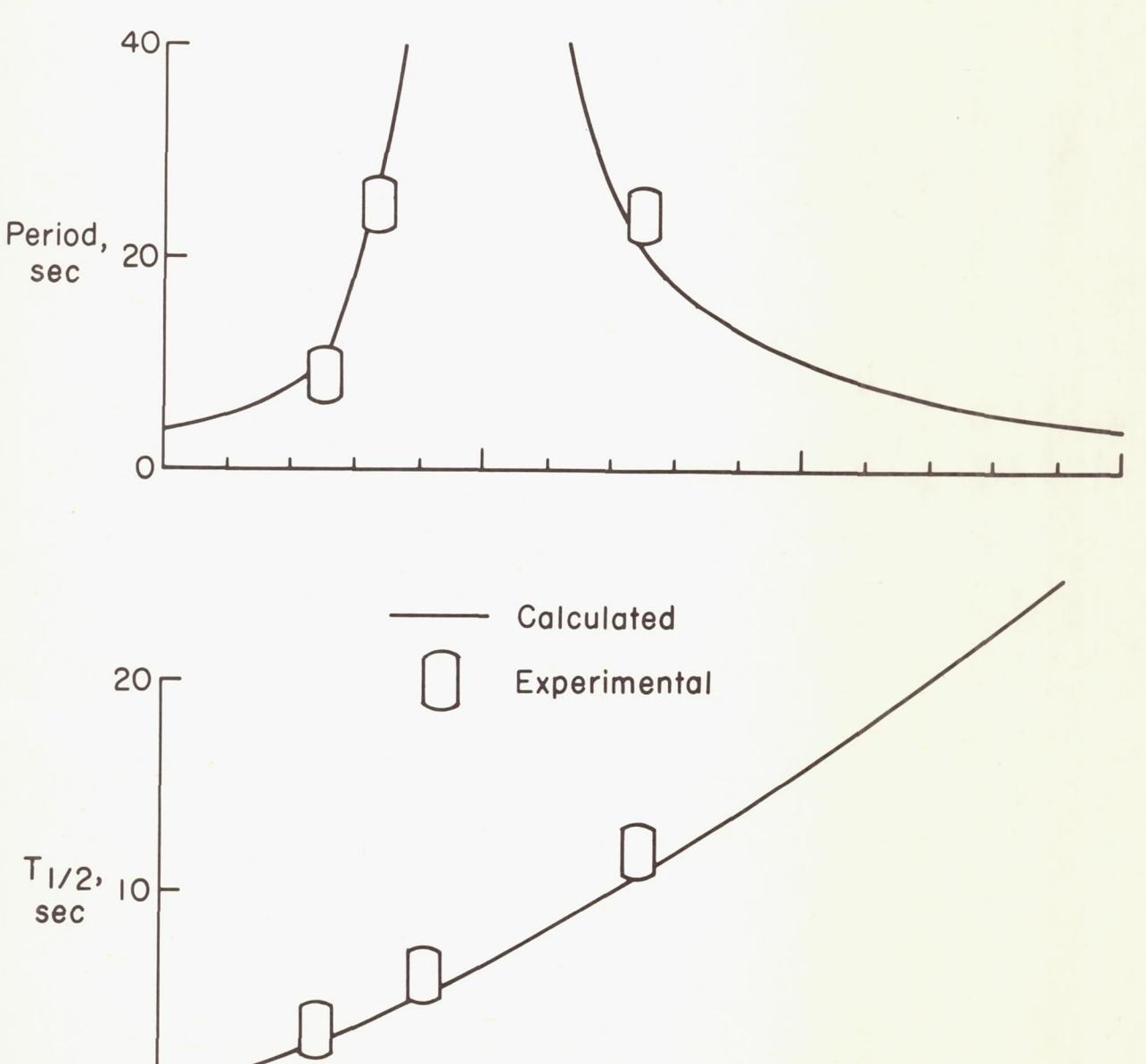

Figure 7.- Comparison of calculated and experimental periods and time to damp to half-amplitude $T_{1/2}$ with a damping gain of 1 second.

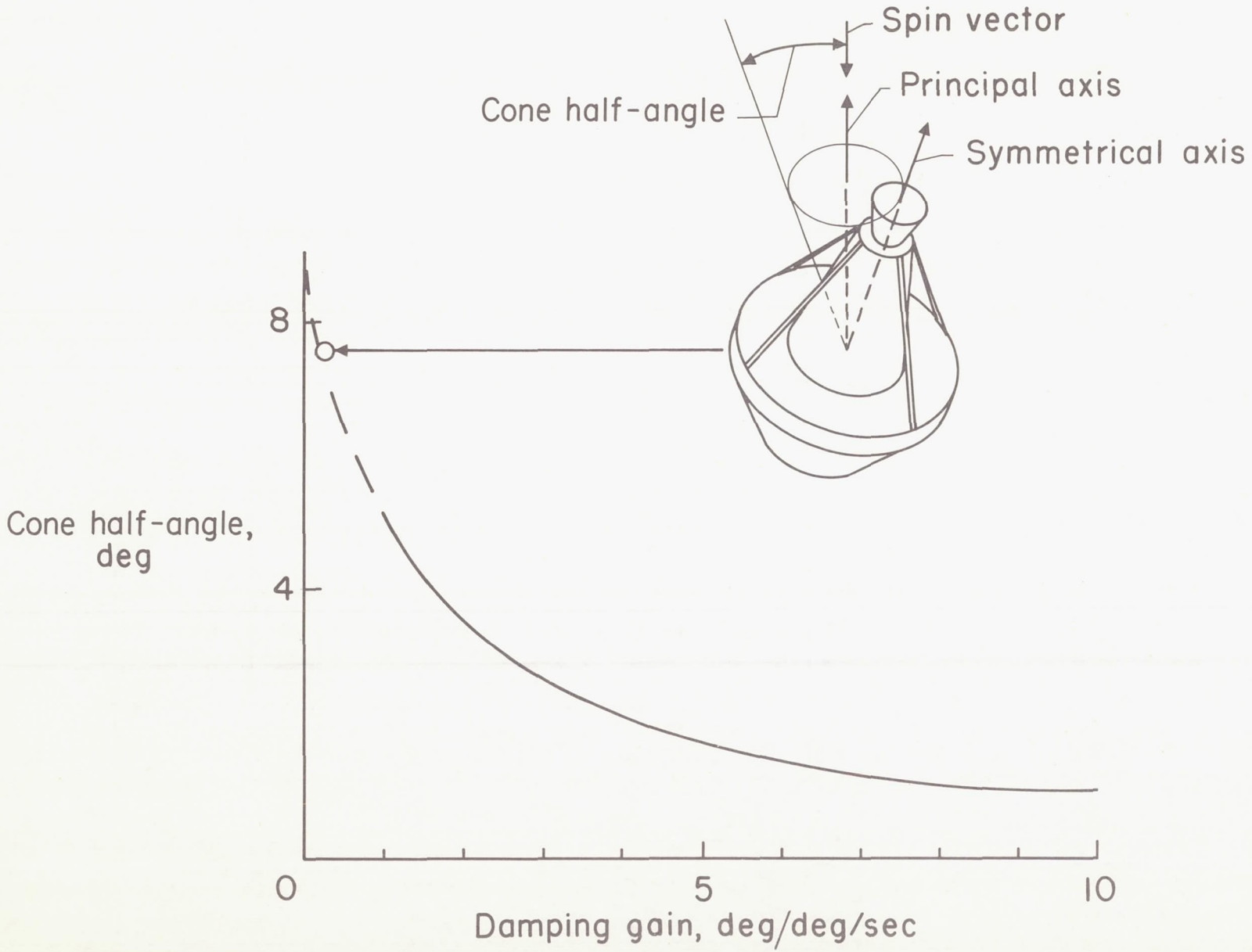

Figure 8.- Variation of steady-state cone half-angle with damping gain for $I_Y/I_X = 0.91$.

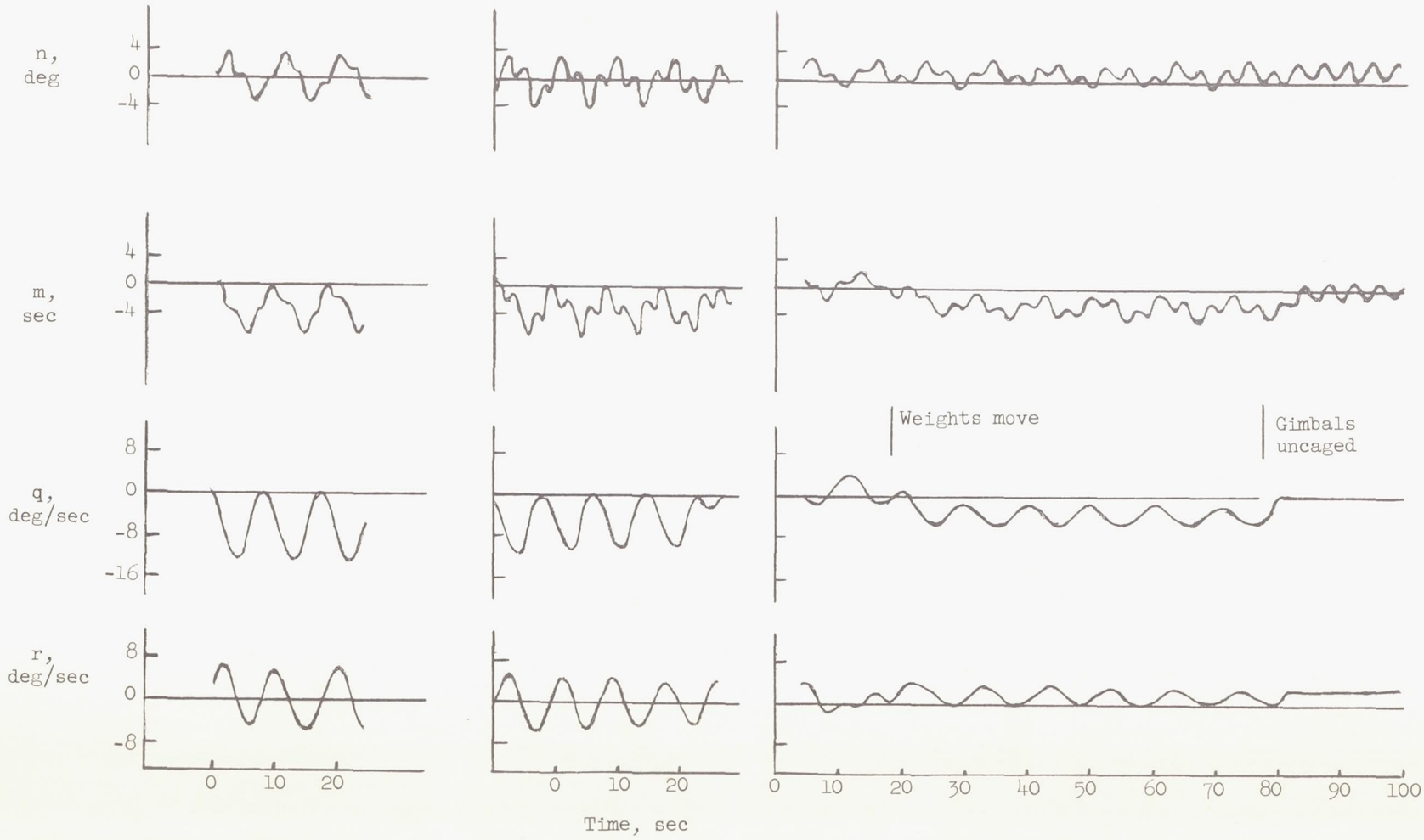

(a) Uncontrolled. (b) Wheel spinning, gimbals uncaged. (c) Programed run.

Figure 9.- Response of simulator with $I_Y/I_X = 0.76$.

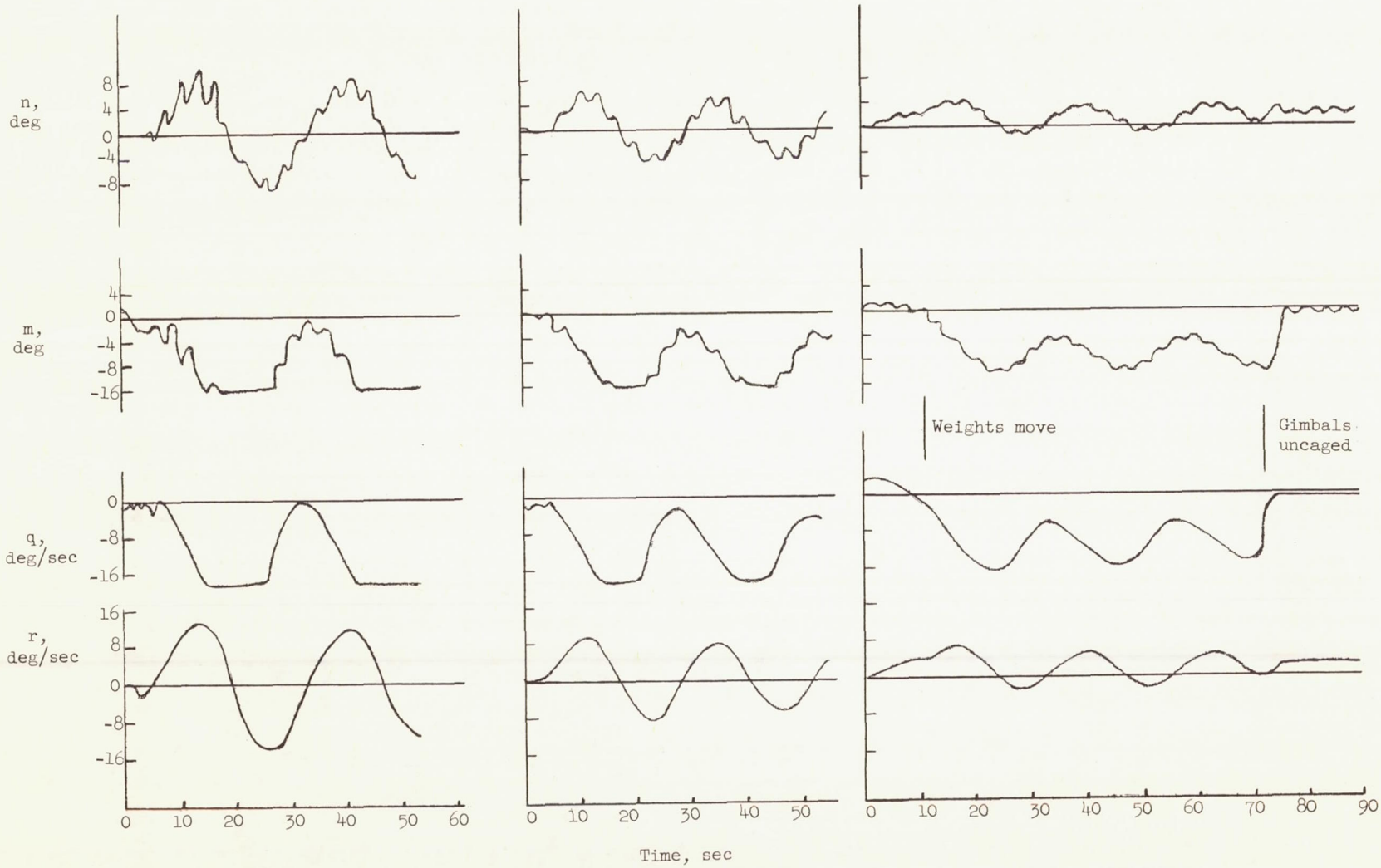

(a) Uncontrolled. (b) Wheel spinning, gimbals caged. (c) Programed run.

Figure 10.- Response of simulator with $I_Y/I_X = 0.91$.

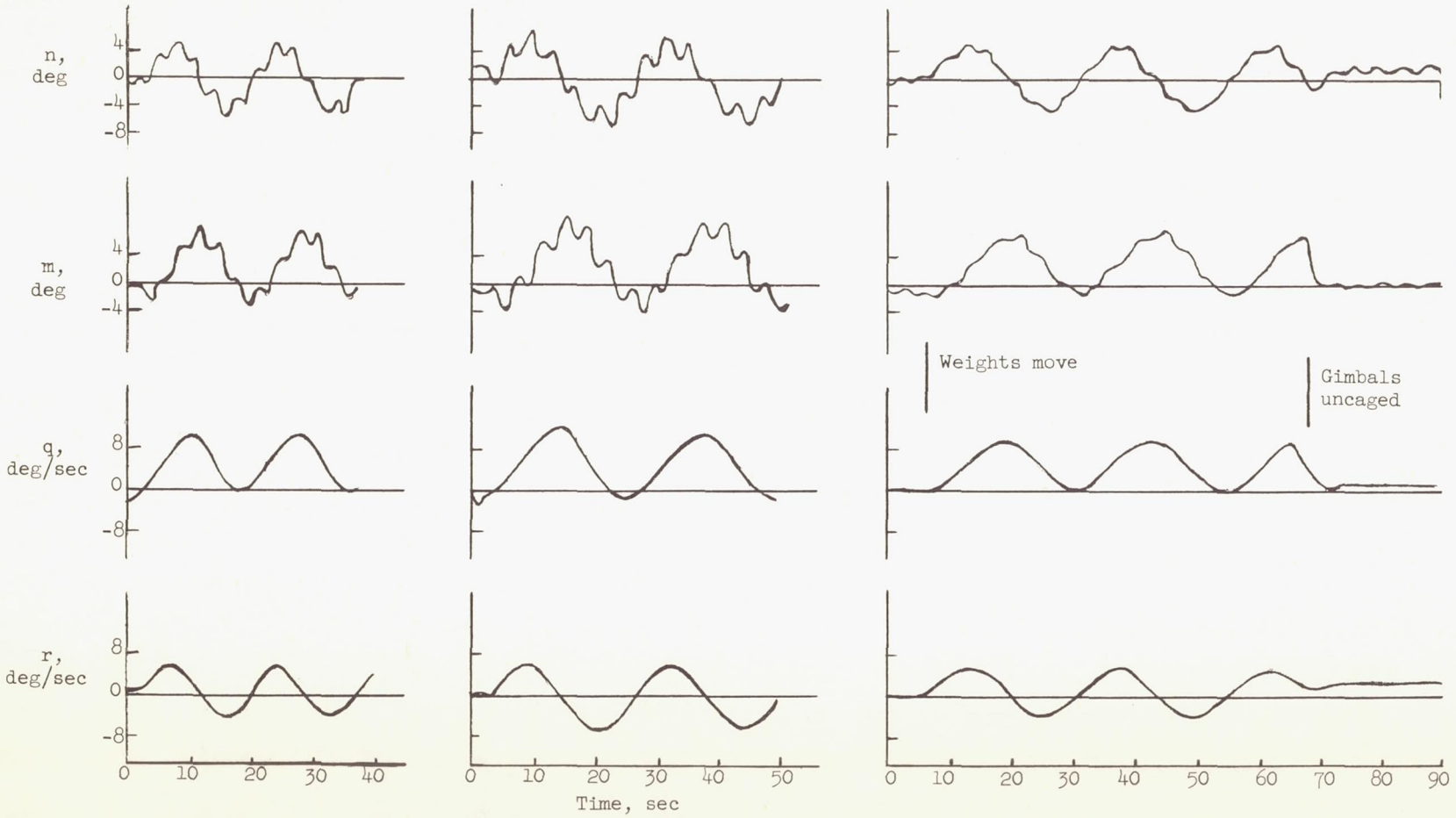

(a) Uncontrolled. (b) Wheel spinning, gimbals caged. (c) Programed run.

Figure 11.- Response of simulator with $I_Y/I_X = 1.25$.

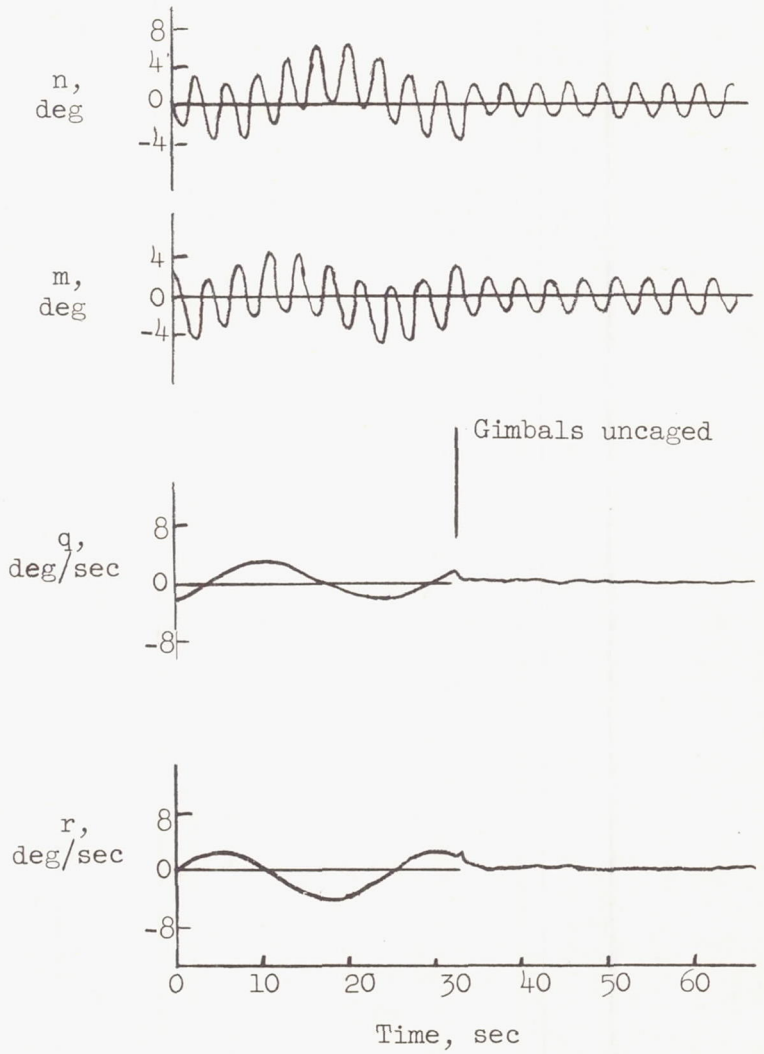

Figure 12.- Response of simulator with both rate-gyro and light-sensor signals used for command.